

13. COMPOSITE DEPTH SCALE AND STRATIGRAPHY FOR SITES 885/886¹

Gerald R. Dickens,² Hilde Snoeckx,² Eve Arnold,³ Joseph J. Morley,⁴ Robert M. Owen,² David K. Rea,² and Lynn Ingram⁵

ABSTRACT

Shipboard whole-core volume magnetic susceptibility records at Holes 885A, 886A, 886B, and 886C were aligned according to sedimentary depth to construct a composite depth scale for Sites 885/886. The composite depth scale then was checked for stratigraphic equivalence at each of the four holes with available polarity chron boundaries and isochronous radiolarian events. Samples from Holes 885A, 886B, and 886C subsequently were analyzed for Ba, Fe, La, and Sc by instrumental neutron activation analysis. Downcore profiles of these elements (as well as results presented in other papers of this volume) indicate the composite depth scale typically allows for intercorrelation to within 0.4 m between holes at Sites 885/886. This composite depth scale has important ramifications toward understanding the stratigraphy of Sites 885/886.

INTRODUCTION

Ocean Drilling Program (ODP) Sites 885/886 are located in the central subarctic Pacific Ocean approximately 60 km south of the Chinook Trough. The two sites are proximal (within 2.3 km), and consist of four holes cored with the advanced hydraulic piston corer (APC): Hole 885A (44°41.296'N, 168°16.319'W), Hole 886A (44°41.384'N, 168°14.416'W), Hole 886B (44°41.384'N, 168°14.416'W), and Hole 886C (44°41.384'N, 168°14.400'W). Drilling disturbance initially was reported as minimal at all four holes (Rea, Basov, Janecek, Palmer-Julson, et al., 1993). Sediment recovered at the holes predominantly consists of variable proportions of clay, diatoms, and Fe-Mn oxyhydroxides (Rea, Basov, Janecek, Palmer-Julson, et al., 1993).

Primary drilling objectives at Sites 885/886 included tracking changes in the accumulation rates of Cenozoic eolian inputs and determining the timing and onset of Neogene siliceous sedimentation in the central North Pacific (Rea, Basov, Janecek, Palmer-Julson, et al., 1993). Realization of these objectives requires accurate placement of age datums and reasonable estimates for the amount of sediment deposited between age datums. It is of interest, therefore, to intercorrelate Holes 885A, 886A, 886B, and 886C according to a composite depth scale such that (1) age datums from one hole may be transferred to an adjacent hole where ages have not yet been determined, and (2) depth offsets, intervals of distortion, and hiatuses can be accounted for (see review in Hagelberg et al., 1995).

PROCEDURE

Individual cores from each hole were adjusted along a composite depth scale such that variations in magnetic susceptibility records occurred at similar depth horizons (magnetic susceptibility records determined by the automated multisensor track were used because they display the largest variability of any high-resolution shipboard measurement at Sites 885/886). Where distances between common points of variation in a single core differed between proximal holes, it was assumed that either (1) the lesser interval represented sedimentary compression and/or contained a hiatus; or (2) the greater interval represented sedimentary expansion. In this paper (in contrast to Murray and

Prell, 1991; Hagelberg et al., 1992), we chose to linearly stretch (or break) lesser intervals such that distances between common points of variation are equivalent at each hole. This choice is favored because the composite sedimentary record at Sites 885/886 is relatively short (a maximum of eight cores at Hole 886C) and because several lengthy (>1.0 m) intervals of nondeposition occur within individual cores. After completing this step, distances between the base and top of successive cores were assumed to be either recovery gaps (positive values) or coring overlaps (negative values). The intercorrelation process, therefore, involved splicing together pieces of different holes to provide a continuous sedimentary record. Such intercorrelation renders a composite record that typically is a different length (often longer) than the length of any hole used to construct the composite record (e.g., Murray and Prell, 1991; Hagelberg et al., 1992, 1995). Hence, depths on the composite record are reported in meters composite depth (mcd) to distinguish them from "true" depths.

Although sedimentary inputs likely were similar through time at these four proximal holes, postdepositional processes may have differed significantly between Hole 885A and the three holes at Site 886. Therefore, we attempted to use magnetic susceptibility datums from cores at Site 886 to construct the composite depth scale; that is, datums at Hole 885A only would be tied to those of Holes 886A, 886B, and 886C subsequent to alignment of holes at Site 886. However, because sediment appears to be missing in Core 145-886C-4H, and because of incomplete recovery of Core 145-886C-5H, intervals from Hole 885A are needed to piece together the entire composite depth scale.

The final steps in our hole intercorrelation involved verification that selected magnetic susceptibility datums were indeed stratigraphically equivalent. This first was accomplished by checking that polarity chron boundaries and isochronous radiolarian events occurred at similar composite depth in each of the four holes. However, because these markers are limited in number and nonexistent in lowermost sediment at Sites 885/886 (Rea, Basov, Janecek, Palmer-Julson, et al., 1993; Morley and Nigrini, this volume), we plotted bulk elemental concentrations downcore in the anticipation that chemical variations at each hole also could be aligned according to composite depth (Heath et al., 1985). It is assumed that downcore variations in geochemistry at each of the four holes record changes in lithology and/or paleoceanography but that these changes are not "time transgressive" over the 2.3 km distance between the four holes.

Bulk sediment Ba, Fe, La, and Sc concentrations were determined on discrete 5-cm samples from all cores at Holes 885A and 886B, and on Cores 145-886C-7H and -8H by instrumental neutron activation analysis (INAA) using the nuclear reactor and counting facilities at the Phoenix Memorial Laboratory, University of Michigan. Individual samples were freeze-dried, homogenized (within a ceramic mortar and

¹ Rea, D.K., Basov, I.A., Scholl, D.W., and Allan, J.F. (Eds.), 1995. *Proc. ODP, Sci. Results*, 145: College Station, TX (Ocean Drilling Program).

² Department of Geological Sciences, University of Michigan, Ann Arbor, MI 48109-1063, U.S.A.

³ Graduate School of Oceanography, University of Rhode Island, Narragansett, RI 02882-1197, U.S.A.

⁴ 32 West End Avenue, Westwood, NJ 07675, U.S.A.

⁵ Department of Geology and Geophysics, University of California, Berkeley, CA 94720, U.S.A.

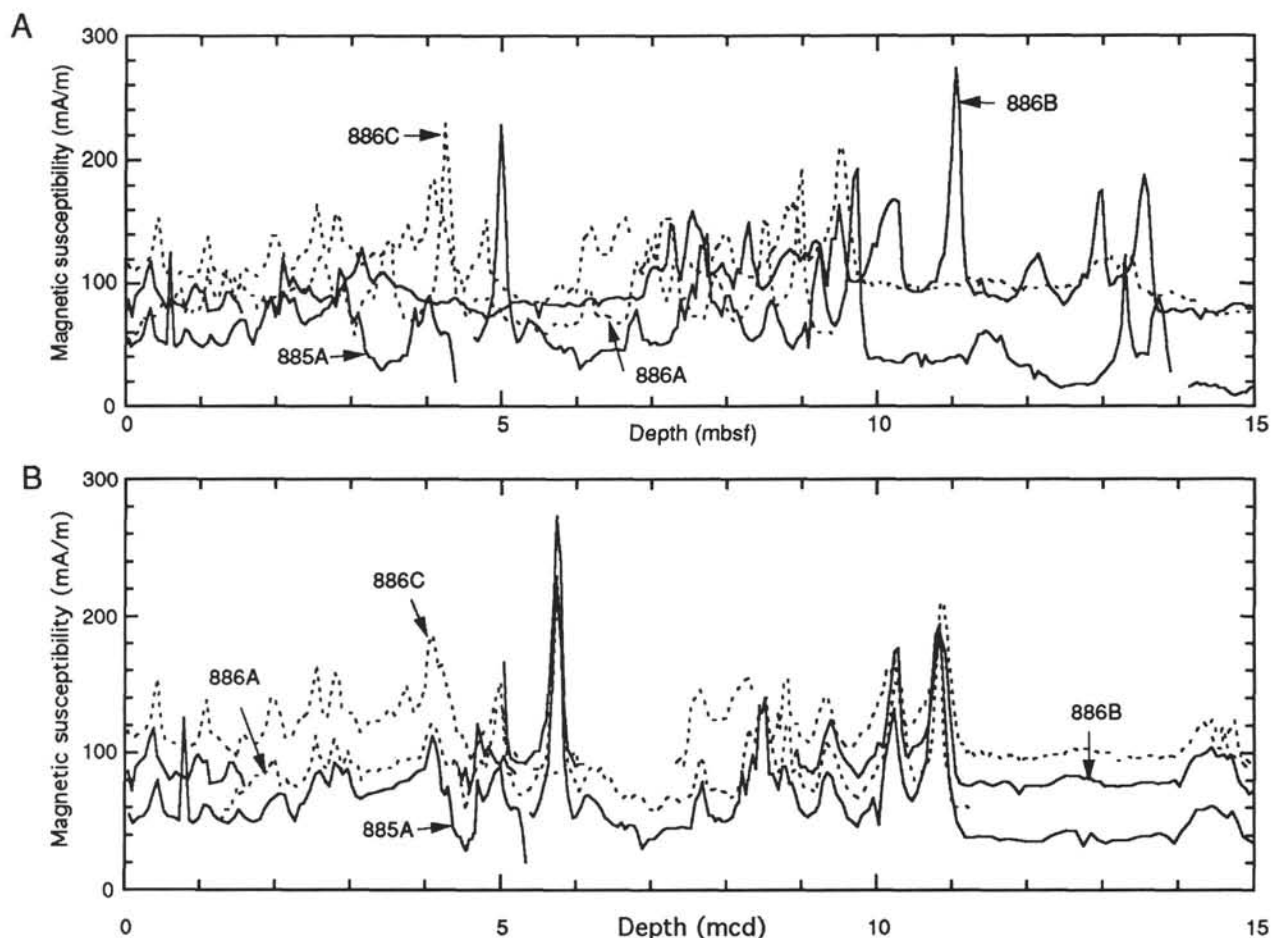


Figure 1. Example demonstrating how cores can be adjusted along a depth scale such that prominent variations in whole-core volume magnetic susceptibility will occur at a similar composite depth. **A.** The magnetic susceptibility records in the upper 15 m at Holes 885A, 886A, 886B, and 886C clearly are not aligned according to meters below seafloor (mbsf). **B.** These records, however, can be aligned according to composite depth (mcd). The magnetic susceptibility records of Holes 886A, 886B, and 886C have been offset by successive 50-mA/m increments for clarity.

pestle), and analyzed as follows. Approximately 250 mg of each sample was enclosed within a prewashed, high-purity quartz tube, irradiated for 20 hr on a rotating holder, counted for 67 min after a decay of 1 week, and analyzed for Ba and La. These same samples were re-counted for 67 min after a decay of 5 weeks, and analyzed for Fe and Sc. Samples received a thermal neutron flux of approximately 5×10^{12} neutrons/cm²/s and were counted using a pair of multiplexed Ge-Li gamma detectors. Gamma lines used for analysis were 496.26, 1099.25, 1596.54, and 889.25 KeV for Ba, Fe, La, and Sc, respectively. Concentrations for all four elements were obtained through standard comparison with NBS-SRM-1633a (coal fly ash), and with half-lives listed in Browne and Firestone (1986). Analytical precision (1σ) typically was less than 4% for analyses of Fe, La, and Sc, and less than 8% for Ba.

RESULTS AND DISCUSSION

Hole Intercorrelation

Downcore variations in magnetic susceptibility at Holes 885A, 886A, 886B, and 886C do not correlate with respect to depth when plotted according to meters below seafloor (mbsf). This depth offset between holes is arrant over the length the sedimentary column (Rea, Basov, Janecek, Palmer-Julson, et al., 1993, p. 313) and pronounced in the upper 15 m (Fig. 1A). However, prominent variations in magnetic susceptibility can be aligned such that they occur at a similar composite depth. Such alignment is demonstrated in detail for the upper 15 m (Fig. 1B) and can be extended to the entire sedimentary

column at Sites 885/886 (Fig. 2). The depths of the magnetic susceptibility datums (to the nearest 0.05 m) that have been used for this procedure are listed in Table 1. The intercorrelation presented here (Fig. 2, Table 1) differs somewhat from that in Rea, Basov, Janecek, Palmer-Julson, et al. (1993, pp. 313, 318). In particular, (1) lowermost sediment at Hole 885A (>50.6 mbsf) is correlated to lowermost sediment at Hole 886C (>71.1 mbsf), (2) the uppermost intense peak at Hole 885A (5.00 mbsf) is correlated to the uppermost intense peaks at Holes 886A (4.25 mbsf) and 886B (11.05 mbsf), and (3) the broad peaks at 13.10 and 16.70 mbsf at Hole 886C are the same peak.

Shipboard determinations of polarity chron boundaries at each of the four holes provide a first check on the suggested magnetic susceptibility alignment. Depths of 13 (of the identified 15) polarity chron boundaries are consistent with hole intercorrelation, inasmuch as their composite depth positions at each hole lie within 0.3 m of one another (Table 2). The Matuyama/Gauss boundary only is aligned to within 0.8 m (Table 2). The likely cause for the misalignment of this polarity chron boundary between Hole 885A and Holes 886B and 886C is discussed below. The polarity chron boundary observed at 51.3 mbsf at Hole 885A is not listed in Table 2 because it clearly is not the onset of C5n.2n as suggested by Rea, Basov, Janecek, Palmer-Julson, et al. (1993, p. 318). Strontium isotopic analyses of fish teeth (Ingram, this volume; Snoeckx et al., this volume) and geochemical/tectonic arguments (Dickens and Owen, this volume) indicate that sediment at this depth at Hole 885A was deposited during the Late Cretaceous rather than during the late Miocene.

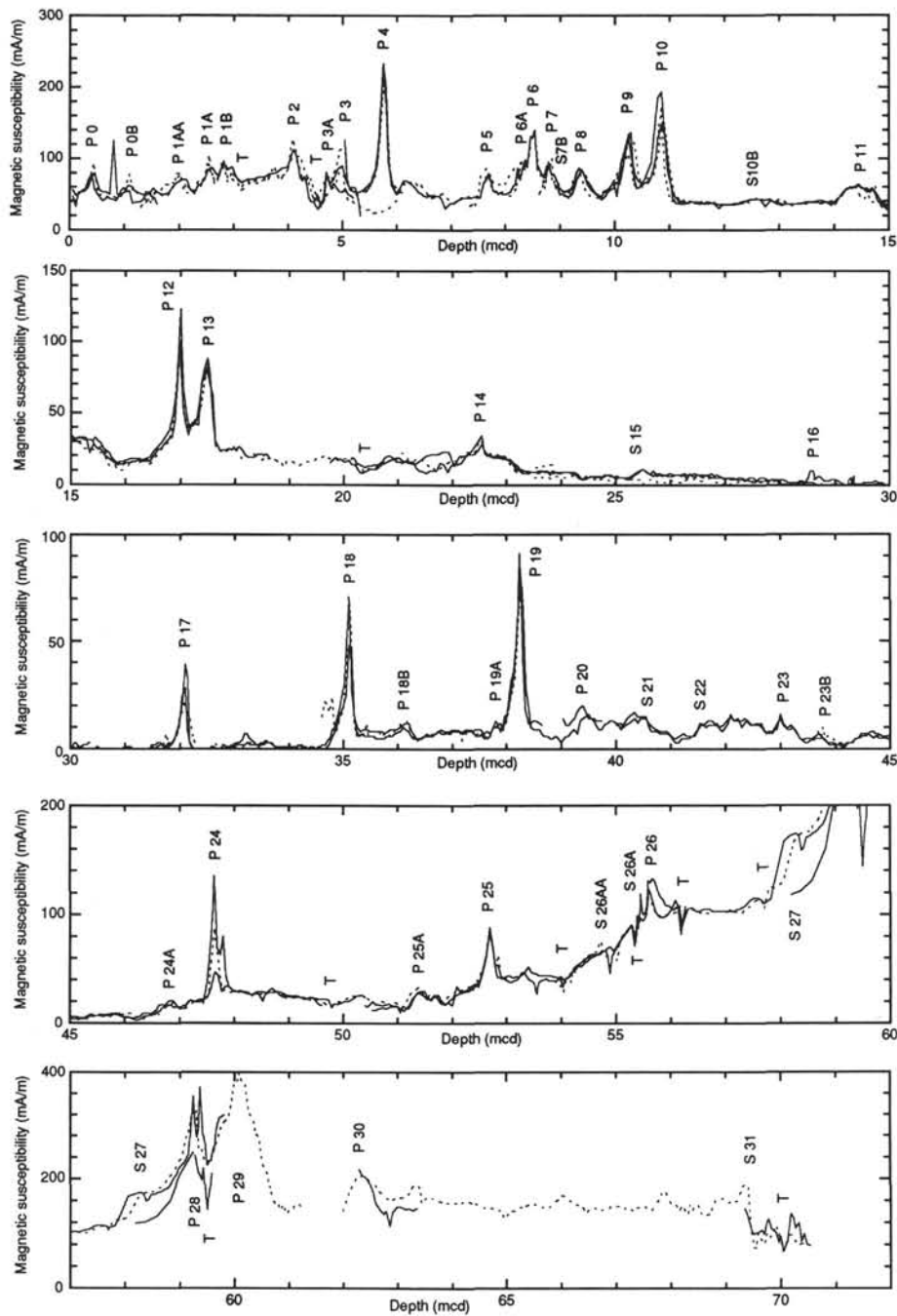


Figure 2. Aligned whole-core volume magnetic susceptibility records for the entire sedimentary column at Sites 885/886. The records at Holes 885A, 886A, 886B, and 886C have been aligned according to datums listed in Table 1 with linear stretching/compression between datums. The “splices” used as references to stretch/compress intervals at other holes are listed in Table 5.

A second evaluation concerning the stratigraphic alignment of magnetic susceptibility datums are downcore changes in radiolarian fauna. Isochronous radiolarian events (first or last occurrences of certain radiolarian species) at Holes 885A and 886C (Morley and Nigrini, this volume) indeed occur at similar composite depth horizons (Table 2). Hence, available time datums (polarity chron boundaries and isochronous radiolarian events) indicate that the composite depth scale is stratigraphically equivalent at all four holes at low resolution within the upper 52 mcd. This is illustrated best by a plot of isochronous datums at two holes according to mcd (Fig. 3).

Downcore bulk concentrations of Ba, Fe, La, and Sc (Table 3) generally support the suggested intercorrelation of Holes 885A, 886B,

and 886C at a much higher resolution. Variations in these elements are aligned to within 0.4 m (Fig. 4), with the exception of three intervals. Between 12 and 15 mcd, depths at Holes 885A and 886B are offset (observed best in the downcore Ba profile). The chemical records at Holes 885A and 886B also are dissimilar at or near 30 mcd. These two discordant depth intervals are discussed below. Sediment between 20 and 22 mcd is intercorrelated poorly as evident in both downcore chemistry and magnetic susceptibility records (Figs. 2 and 4), but a better alignment on the basis of prominent magnetic susceptibility datums is not obvious.

Importantly, bulk chemistry analyses support the proposed correlation of magnetic susceptibility variations in lowermost sediment at

Table 1. Magnetic susceptibility datums used to intercorrelate holes at Sites 885/886.

Datum	Depth (mbsf)				Depth (mcd)
	Hole 885A	Hole 886A	Hole 886B	Hole 886C	
Peak 0	0.35		0.35	0.40	0.40
Peak 0B	0.80	TH	1.05	1.10	1.10
Peak 1AA	1.55	0.75	?	2.00	2.00
Peak 1A	1.90	1.10	RG	2.55	2.55
Peak 1B	2.10	1.35	RG	2.80	2.80
Trough	2.40	1.75	RG	3.15	3.15
Peak 2	2.85	2.60	RG	4.10	4.10
Trough	3.40	3.05	2.00	4.50	4.55
Peak 3A	3.85	3.20	2.10	?	4.70
Peak 3	4.05	3.50	2.25?, 10.25	4.80	5.00
Peak 4	5.00	4.25	11.05	?	5.75
Peak 5	6.75	6.15	RG	6.20	7.65
Peak 6A	7.40	6.80	RG	6.65	8.30
Peak 6	7.70	7.00	RG	7.20	8.50
Peak 7	8.05	7.30	RG	7.20	8.80
Step 7B	8.15?	7.45	11.40	7.50	8.95
Peak 8	8.60	7.85	12.10	8.00	9.35
Peak 9	9.25	8.50	12.95	8.90	10.25
Peak 10	9.75	9.00	13.55	9.50	10.85
Step 10B	10.50	EH	14.70	11.20	12.55
Peak 11	11.45		16.10	13.10, 16.70	14.45
Peak 12	13.30		18.65	18.95	17.00
Peak 13	13.75		19.15	19.40	17.50
Trough	14.80		?	22.30	20.40
Peak 14	15.85		22.80	24.45	22.55
Step 15	18.80		25.05	?	25.50
Peak 16	21.85		?	30.15	28.55
Peak 17	26.55		32.40	33.70	32.10
Peak 18	30.00		35.40	35.85	35.10
Peak 18B	30.95		36.40	37.10	36.10
Peak 19A	32.45		38.10	39.15	37.80
Peak 19	33.00		38.55	39.70	38.25
Peak 20	33.60		39.70	NR	39.40
Step 21	34.75		40.40	NR	40.55
Step 22	35.55		41.40	NR	41.55
Peak 23	36.60		42.85	NR	43.00
Peak 24A	39.85		46.70	48.35	46.90
Peak 24	40.50		47.50	49.05	47.65
Trough	42.05		RG	51.15	49.75
Peak 25A	43.65		50.00	52.80	51.40
Peak 25	44.65		50.95	54.10	52.70
Trough	46.15		52.30	55.55	54.05
Step 26AA	46.90		?	56.80	54.70
Step 26A	47.50		53.50	57.80	55.25
Trough	47.75		53.60	57.95	55.35
Peak 26	48.10		54.45	58.20	55.60
Trough	48.60		55.25	58.80	56.20
Trough	?		56.45	60.30	57.70
Step 27	48.70		56.70	60.80	58.20
Peak 28	48.95		57.80	61.85	59.25
Trough	49.35		58.30	62.10	59.50
Peak 29	NR		NR	62.70	60.10
Peak 30	49.55		NR	64.15	62.30
Step 31	50.65		NR	71.20	69.35
Trough	51.45		NR	71.90	70.05
Basalt contact	52.30		68.80	EH	70.90

Notes: Identification of magnetic susceptibility datums shown in Figure 2. Depths of magnetic susceptibility datums reported to the nearest 0.05 m. TH = top of hole, EH = end of hole, RG = recovery gap, and NR = not recovered.

Holes 885A and 886C (in contrast to Rea, Basov, Janecek, Palmer-Julson, et al., 1993, p. 313). Shipboard work suggested that the peak (our Peak 30) at 49.55 mbsf and trough at 51.45 mbsf at Hole 885A were aligned to the peak (our Peak 29) at 62.70 mbsf and trough at 63.60 mbsf at Hole 886C. Although these shipboard interpretations are acceptable on the basis of magnetic susceptibility values, they clearly are inconsistent with bulk chemistry (particularly Fe and La concentrations; Table 3, Fig. 4).

Changes in rock magnetic parameters (fig. 1 in Arnold et al., this volume) and weight percentage of extracted component (fig. 4 in Snoeckx et al., this volume) are aligned to within 0.4 m, excluding the aforementioned intervals between 12 and 30 mcd.

Stratigraphic Implications of the Composite Depth Scale

Assuming similar sedimentation rates at Holes 885A, 886A, 886B, and 886C, the suggested intercorrelation of these holes implies that

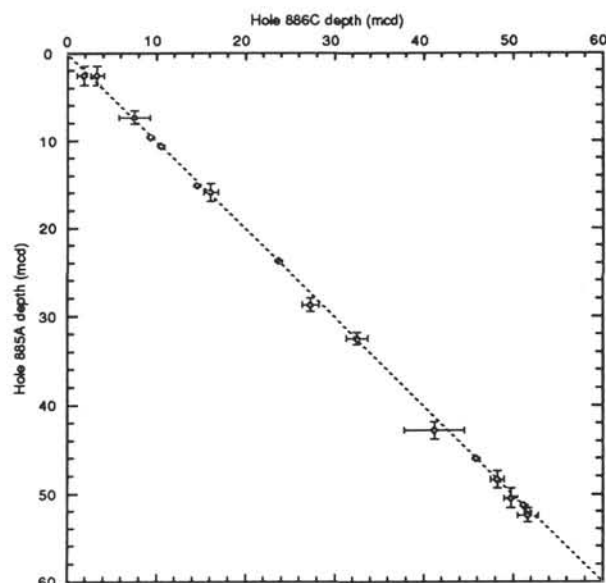


Figure 3. Plot of polarity chron boundaries and isochronous radiolarian events at Holes 885A and 886C according to composite depth (mcd). As evident by all data positioned on a line with an origin (0, 0 mcd) and slope = 1, the two holes are aligned such that they are stratigraphically equivalent. Error bars for depths of polarity chron boundaries are assumed to be 0.10 m, whereas those for radiolarian events are assumed to be the sampling distance in which the event occurs.

recovery gaps range from 0.10 to 2.85 m at Sites 885/886 (Table 4, Fig. 5). Several coring overlaps also occur, and these range from 0.10 to 3.60 m (Table 4, Fig. 5). The range of depth offsets (including both gaps and overlaps) is similar to that observed at sites drilled during ODP Leg 138 (Hagelberg et al., 1992) and other sites drilled during Leg 145 (Rea, Basov, Janecek, Palmer-Julson, et al., 1993) with the notable exception of the 3.60 m overlap between Cores 145-886C-2H and -3H. Three of the core breaks are associated with minor drilling disturbance (<25 cm in length), but only the overlap between Cores 145-886C-6H and -7H occurs in highly disturbed sediment (Table 4). Thus, the proposed 3.60 m coring overlap at Hole 886C might seem spurious. However, although we cannot explain its origin, this lengthy overlap is supported by a 3.0 to 4.5 m repetition of radiolarian fauna assemblages in the lowermost three sections of Core 145-886C-2H and the uppermost three sections of Core 145-886C-3H (Morley and Nigrini, this volume). The above depth offsets at core breaks only can be offered as rough estimates because postdepositional processes at these holes were dissimilar (i.e., there are intervals within cores in which the length of sediment at one or more holes is significantly less than at other holes, see below).

The break between Cores 145-886C-7H and -8H has no adjacent hole in which to determine depth offset; however, the significant change in chemistry (Table 3) across this core break suggests either a recovery gap and/or the presence of a hiatus. On the basis of modeling the flux of hydrothermal materials to this lowermost sediment, Dickens and Owen (1993) initially estimated that a recovery gap of approximately 0.75 m spanned this core break. This model did not include the possibility that a prominent hiatus might exist at or near the core break (as suggested by strontium isotopic analyses of fish teeth, see below). Thus, although this 0.75 m recovery gap has been retained for construction of the composite depth scale, it must be regarded as an arbitrary value.

The interval surrounding 30 mcd (within the core of the "diatom dump"; >95 % biogenic silica, Snoeckx et al., this volume) poses an intercorrelation problem: there is a paucity of magnetic susceptibility information at Holes 885A, 886B, and 886C; the bottom of Core 145-886B-4H was not recovered (including possibly, Peak 16); and

Table 2. Composite depths for polarity chron boundaries and isochronous radiolarian events at Sites 885/886.

Boundary or event	Datum	Age (Ma)	Depth (mcd)			
			Hole 885A	Hole 886A	Hole 886B	Hole 886C
R	LO <i>S. acquilonium</i>	0.4	1.52–3.67			1.14–2.64
R	LO <i>S. universon</i>	0.55	1.52–3.67			2.64–4.14
P	Brunhes/Matuyama	0.78	4.85	4.88		
P	Termination Jaramillo	0.98	5.70	5.71		
P	Onset Jaramillo	1.05	6.14	6.20		
R	LO <i>L. heteroporos</i>	1.7	6.56–8.10			5.84–9.30
P	Termination Olduvai	1.76	9.59	9.55		9.38
P	Onset Olduvai	1.98	10.60	10.52		10.53
P	Matuyama/Gauss	2.60	15.14	14.58	14.60	
R	FO <i>C. davisiana davisiana</i>	2.9	14.86–16.93		15.29–16.99	
P	Gauss/Gilbert	3.55	23.75	23.61	23.75	
R	LO <i>D. bullatus</i>	4.2	27.95–29.45		26.40–28.29	
R	LO <i>S. peregrina</i> (see below)	~5.0	31.80–33.14			31.34–33.75
P	Termination C3An.1n	5.71	35.48	35.46		
P	Onset C3An.1n	5.95	37.05	37.31		
P	Termination C3An.2n	6.08	38.49			
P	Onset C3An.2n	6.38	40.61			
R	FO <i>L. heteroporos</i>	6.5	41.83–43.78			37.90–44.63
P	Termination C4n.1n	7.25	45.98	46.11	45.89	
R	<i>T. S. delmontensis</i> – <i>S. peregrina</i>	7.55	47.35–49.34			47.51–49.04
R	FO <i>S. acquilonium</i>	7.7	49.34–51.57			49.04–50.54
P	Onset C4n.2n	7.89	51.30			51.25
P	Termination C4An	8.53	52.01			51.72
R	LO <i>L. nipponica magnacornuta</i>	8.8	51.57–53.24			50.54–52.90

Notes: Ages and unconverted depths (mbsf) for polarity chron boundaries (P) and radiolarian events (R) are found in Rea, Basov, Janecek, Palmer-Julson, et al. (1993) and Morley and Nigrini (this volume). For radiolarian events, LO = last occurrence, FO = first occurrence, and T = species transition. The LO of *S. peregrina* is diachronous throughout the North Pacific (Morley and Nigrini, this volume), but is assumed to be isochronous at Sites 885/886.

core breaks occur at Holes 885A and 886B. We have chosen to use Hole 886C to construct the composite record across this interval because it does not contain a core break. This interpretation implies coring overlaps between Cores 145-885A-3H and -4H (1.15 m), and between Cores 145-886B-4H and -5H (0.75 m). However, Core 145-886C-4H appears to be compressed by up to 1.5 m on the basis of lengths between available magnetic susceptibility peaks. Intercorrelation between holes at or near 30 mcd, therefore, may be off by up to 1.5 m. Indeed, studies concerning sedimentation rates should consider the possibility that some degree of compression may have occurred at all holes at or near 30 mcd as a result of drilling through soft diatom ooze.

In addition to expected depth offsets between successive cores, the intercorrelation of Holes 885A, 886A, 886B, and 886C presented here has several important implications concerning the stratigraphy of Sites 885/886 (Table 4, Fig. 5).

First, the middle portion of Core 145-886B-2H is a conundrum. Between 2.60 and 10.25 mbsf, no obvious correlation is present between the magnetic susceptibility record at Hole 886B and the records observed at the other three holes. This correlation problem also is apparent in comparison of downcore magnetic inclination records (Rea, Basov, Janecek, Palmer-Julson, et al., 1993, p. 312). Because inclusion of this 7.50 m depth interval renders unreasonable linear sedimentation rates at Hole 886B, we conclude that it is "extra" sediment (i.e., sediment is not "missing" at the other three holes). However, because this interval does not appear to be "flow in," a slump deposit, or a repeated section, the origin of this interval remains inexplicable. We suggest that future investigations avoid the middle portion of Core 145-886B-2H until a good hypothesis concerning its origin is forwarded.

Second, a hiatus exists at Hole 886C between 4.80 and 6.10 mbsf, and represents 1.25 m of depth offset relative to the composite sedimentary record. The hiatus is observed in the sedimentary column by gradational and sharp contacts between 5.86 and 6.10 mbsf (Rea, Basov, Janecek, Palmer-Julson, et al., 1993), and also is inferred from radiolarian fauna assemblages by the limited depth range of *Eucyrtidium matuyamai* (Morley and Nigrini, this volume). This particular hiatus at Hole 886C appears to be hole specific.

Third, the interval between 9.75 and 15.85 mbsf at Hole 885A is greatly compressed relative to stratigraphically equivalent sediment

at Holes 886B and 886C, and represents 5.60 m of depth offset between Hole 885A and the composite sedimentary record. Although up to 1.85 m can be accounted for by a recovery gap between Cores 145-885B-2H and -3H, portions of this interval (1) were deposited more slowly than at Site 886, (2) have been compressed during drilling, and/or (3) contain multiple hiatuses. The latter two possibilities seem more reasonable given the proximity of Sites 885 and 886 to each other. However, because drilling disturbance and/or sedimentary contacts are not evident in this interval at Hole 885A, available data prevent discrimination between any of these possibilities. Moreover, the aforementioned misalignment of the Matuyama/Gauss boundary and bulk chemistry values suggests that simple linear stretching of the sediment in the "compressed" interval at Hole 885A is not valid.

Fourth, Sections 145-885A-6H-5 and -6H-6 contain three conspicuous hiatuses. Based upon a combination of the results from magnetic susceptibility and bulk chemistry analyses, these hiatuses occur between 48.65 and 48.70 mbsf, 49.41 and 49.55 mbsf, and 50.40 and 50.65 mbsf, and represent approximately 2.00, 1.90, and 5.95 m, respectively, of "missing" sediment relative to Holes 886B and/or 886C. A color change (apparent in color photographs but not described in core barrel sheets) is observed at approximately 50.30 mbsf at Hole 885A; this color variation likely marks the lower of the three hiatuses. Although a color change and/or a sedimentary contact is not observed for either of the upper two hiatuses, ages determined from strontium isotopic analyses of fish teeth (Ingram, this volume; Snoeckx et al., this volume) are consistent with such an interpretation, inasmuch as they indicate that >10 m.y. of sedimentation is missing between 44.60 and 47.60 mbsf, and that >25 m.y. of sedimentation is missing between 49.10 and 52.10 mbsf. Evidence provided by strontium isotopic analyses further suggests that the upper two hiatuses are present at Site 886. Lengthy (>10 m.y.) gaps in the sedimentary record occur between 54.27 and 55.05 mbsf at Hole 886B, and between 57.15 and 58.65 mbsf, and 61.90 and 68.15 mbsf at Hole 886C (Ingram, this volume; Snoeckx et al., this volume). The depth interval of the composite record between approximately 55 and 62 mcd therefore represents a time where hiatuses occur at both Sites 885 and 886, but where more sediment effectively was removed at Hole 885A than at Holes 886B and 886C. The roughly exponential decrease in hydrothermal deposition through time at Hole 886C (Dickens and Owen, this volume), however, does suggest that Core 145-886C-8H

Table 3. Elemental concentrations for samples from Holes 885A, 886B, and 886C.

Core, section, interval (cm)	Depth (mbsf)	Depth (mcd)	Ba (ppm)	La (ppm)	Fe (%)	Sc (ppm)	Core, section, interval (cm)	Depth (mbsf)	Depth (mcd)	Ba (ppm)	La (ppm)	Fe (%)	Sc (ppm)
145-885A-							1H-CC, 5-10	1.63	1.68	1,184	27.6	4.35	20.35
1H-1, 5-10	0.05	0.06	2,177	30.4	4.66	23.86	2H-1, 5-10	1.85	4.45	3,811	22.7	3.17	18.24
1H-1, 80-85	0.80	1.10	1,269	28.5	4.71	23.14	2H-1, 80-85	2.60	5.20	1,658	35.9	4.75	22.20
1H-2, 5-10	1.55	2.00	973	28.6	4.64	22.27	2H-6, 105-110	10.35	5.09	1,663	36.5	4.78	21.29
1H-2, 80-85	2.30	3.03	2,084	28.9	4.61	23.32	2H-7, 5-10	10.85	5.56	2,147	34.2	4.90	24.54
1H-3, 5-10	3.05	4.22	1,784	28.8	4.76	24.52	2H-7, 30-35	11.10	5.80	1,905	28.1	4.91	24.44
1H-3, 80-85	3.80	4.67	2,870	22.2	3.78	20.62	3H-1, 30-35	11.60	9.07	2,141	34.0	4.55	23.57
1H-CC, 5-10	4.45	5.40	1,889	32.8	4.87	25.20	3H-1, 80-85	12.10	9.37	1,852	28.1	4.79	24.53
2H-1, 5-10	4.65	5.40	1,802	33.5	4.98	23.61	3H-2, 5-10	12.85	10.14	3,408	21.8	4.23	25.28
2H-1, 80-85	5.40	6.18	1,953	31.7	5.04	24.86	3H-2, 80-85	13.60	10.92	3,094	21.0	4.79	26.76
2H-2, 5-10	6.15	7.00	2,234	32.0	4.59	24.13	3H-3, 5-10	14.35	11.98	4,925	30.7	4.05	24.76
2H-2, 80-85	6.90	7.78	3,041	28.6	4.49	26.28	3H-3, 80-85	15.10	13.04	4,685	31.7	4.10	25.20
2H-3, 5-10	7.65	8.46	2,796	20.1	4.79	26.19	3H-4, 5-10	15.85	14.10	5,483	27.7	3.99	24.64
2H-3, 80-85	8.40	9.15	2,254	30.5	4.53	24.46	3H-4, 80-85	16.60	14.95	6,612	26.0	3.51	23.86
2H-4, 5-10	9.15	10.11	3,196	22.7	4.65	26.68	3H-4, 105-110	16.85	15.20	5,712	30.3	3.34	24.51
2H-4, 80-85	9.90	11.19	5,023	30.2	4.11	26.10	3H-5, 5-10	17.35	15.70	2,329	4.8	0.50	3.85
2H-5, 5-10	10.65	12.85	6,157	30.5	3.95	24.42	3H-5, 30-35	17.60	15.95	4,734	12.1	1.15	11.78
2H-5, 80-85	11.40	14.35	5,408	27.7	4.11	25.11	3H-5, 55-60	17.85	16.20	3,776	15.5	1.16	12.74
2H-6, 5-10	12.15	15.41	4,510	32.7	3.23	23.75	3H-5, 80-85	18.10	16.45	5,312	13.9	1.79	14.66
2H-6, 30-35	12.40	15.76	3,257	11.9	1.19	12.16	3H-5, 105-110	18.35	16.70	6,275	17.5	2.80	19.35
2H-6, 80-85	12.90	16.45	6,532	16.3	2.01	16.19	3H-6, 5-10	18.85	17.20	3,196	20.5	2.97	20.51
2H-7, 5-10	13.65	17.39	6,133	23.8	3.70	25.38	3H-6, 80-85	19.60	17.95	3,189	19.2	2.53	22.04
3H-1, 5-10	14.15	19.75	3,298	17.1	2.31	17.90	3H-6, 105-110	19.85	18.20	3,797	23.0	2.70	21.31
3H-1, 80-85	14.90	20.60	2,112	15.7	1.59	14.27	4H-1, 5-10	20.85	20.15	4,305	21.2	2.20	18.17
3H-2, 5-10	15.65	22.14	3,538	25.3	2.19	17.36	4H-1, 80-85	21.60	21.03	4,390	18.4	2.15	19.25
3H-2, 80-85	16.40	23.10	5,918	16.2	1.50	12.20	4H-2, 5-10	22.35	21.98	4,713	23.1	2.01	18.06
3H-2, 105-110	16.65	23.35	3,534	12.4	1.05	9.34	4H-2, 30-35	22.60	22.30	3,655	20.9	2.34	19.75
3H-3, 5-10	17.15	23.85	3,924	9.8	1.34	10.69	4H-2, 80-85	23.10	22.94	4,825	21.0	2.18	17.87
3H-3, 80-85	17.90	24.60	2,512	7.9	0.79	6.71	4H-2, 105-110	23.35	23.27	4,420	15.1	1.24	10.74
3H-3, 105-110	18.15	24.85	2,946	6.8	0.87	6.85	4H-2, 130-135	23.60	23.60	2,701	16.4	0.80	10.52
3H-4, 5-10	18.65	25.35	3,045	5.9	0.70	6.56	4H-3, 5-10	23.85	23.93	4,493	10.6	1.04	9.26
3H-4, 80-85	19.40	26.10	2,990	7.0	0.88	7.44	4H-3, 30-35	24.10	24.25	1,287	6.3	0.67	6.31
3H-5, 5-10	20.15	26.85	2,197	9.1	0.67	6.85	4H-3, 80-85	24.60	24.91	3,262	8.1	0.97	7.55
3H-5, 80-85	20.90	27.60	2,365	4.5	0.54	5.13	4H-3, 105-110	24.85	25.24	2,389	4.2	0.55	5.74
3H-6, 5-10	21.65	28.35	2,398	5.7	0.40	4.28	4H-4, 5-10	25.35	25.80	2,803	7.8	0.91	6.96
3H-6, 80-85	22.40	29.10	2,832	6.1	0.48	4.43	4H-4, 80-85	26.10	26.55	1,778	7.8	0.79	5.97
3H-7, 5-10	23.15	29.85	2,413	3.9	0.28	3.67	4H-5, 5-10	26.85	27.30	2,696	5.9	0.65	4.81
4H-1, 5-10	23.65	29.20	2,823	7.0	0.24	4.24	4H-5, 80-85	27.60	28.05	2,471	4.4	0.80	4.31
4H-1, 85-90	24.45	30.00	2,237	3.2	0.39	3.92	4H-6, 5-10	28.35	28.80	1,933	3.5	0.24	3.30
4H-2, 5-10	25.15	30.70	1,958	3.2	0.22	3.58	4H-6, 80-85	29.10	29.55	2,477	6.2	0.68	5.90
4H-2, 85-90	25.95	31.50	3,566	5.7	0.63	6.24	5H-1, 5-10	30.35	30.05	2,955	5.8	0.38	6.12
4H-3, 5-10	26.65	32.19	4,379	7.1	0.77	7.06	5H-1, 80-85	31.10	30.80	2,035	3.3	0.39	3.42
4H-3, 85-90	27.45	32.88	5,193	13.5	1.40	13.25	5H-2, 5-10	31.85	31.55	3,448	5.4	0.45	6.18
4H-4, 5-10	28.15	33.49	5,985	12.5	1.77	13.20	5H-2, 80-85	32.60	32.30	3,826	9.2	0.52	5.51
4H-4, 85-90	28.95	34.19	3,822	10.7	1.12	11.95	5H-3, 5-10	33.35	33.05	5,979	15.8	1.74	15.02
4H-5, 5-10	29.65	34.80	4,477	10.1	1.23	9.07	5H-3, 30-35	33.60	33.30	5,631	14.4	0.75	10.78
4H-5, 85-90	30.45	35.60	5,841	12.2	1.10	10.81	5H-3, 80-85	34.10	33.80	4,265	11.4	1.04	9.75
4H-5, 105-110	30.75	35.93	6,036	15.5	1.14	11.17	5H-4, 5-10	34.85	34.55	3,796	7.9	0.98	8.42
4H-6, 5-10	31.15	36.37	5,288	8.2	0.91	8.79	5H-4, 80-85	35.60	35.30	3,903	11.9	1.29	11.51
4H-6, 85-90	31.95	37.25	3,268	6.8	0.74	7.67	5H-4, 105-110	35.85	35.55	5,060	13.4	0.73	9.89
4H-7, 5-10	32.65	37.96	4,077	10.2	0.98	8.43	5H-5, 5-10	36.35	36.05	5,735	12.6	1.65	12.80
5H-1, 5-10	33.15	38.95	5,685	18.9	2.28	19.97	5H-5, 80-85	37.10	36.80	2,630	8.7	1.10	9.83
5H-1, 80-85	33.90	39.70	5,857	19.8	1.73	17.47	5H-6, 5-10	37.85	37.55	3,497	8.0	0.23	5.53
5H-2, 5-10	34.65	40.45	7,204	19.2	1.86	15.96	5H-6, 80-85	38.60	38.30	2,749	9.2	1.79	11.95
5H-2, 30-35	34.90	40.74	4,881	13.9	0.69	10.02	5H-7, 5-10	39.35	39.05	3,121	13.5	1.45	11.86
5H-2, 80-85	35.40	41.36	2,378	9.9	0.94	9.05	6H-1, 5-10	39.85	40.00	5,867	18.1	2.05	17.61
5H-2, 105-110	35.65	41.69	2,994	15.4	1.25	12.23	6H-1, 30-35	40.10	40.25	6,907	17.5	1.37	14.76
5H-3, 5-10	36.15	42.38	2,970	17.7	1.77	13.82	6H-1, 80-85	40.60	40.75	3,678	9.8	0.93	10.58
5H-3, 30-35	36.40	42.72	3,183	12.6	0.86	9.75	6H-2, 5-10	41.35	41.50	2,976	17.4	1.61	12.90
5H-3, 80-85	36.90	43.36	3,414	11.2	0.98	7.73	6H-2, 80-85	42.10	42.25	3,928	16.0	1.70	13.76
5H-3, 105-110	37.15	43.66	2,397	9.1	0.57	7.42	6H-3, 5-10	42.85	43.00	2,186	21.0	2.37	15.68
5H-4, 5-10	37.65	44.25	2,648	10.2	0.69	5.63	6H-3, 80-85	43.60	43.75	1,853	8.5	0.72	6.74
5H-4, 80-85	38.40	45.15	2,115	5.2	0.65	5.73	6H-4, 5-10	44.35	44.50	2,334	7.7	0.96	7.32
5H-5, 5-10	39.15	46.04	2,537	9.3	1.15	8.73	6H-4, 80-85	45.10	45.25	3,323	6.7	0.64	7.00
5H-5, 80-85	39.90	46.93	3,947	18.8	1.82	15.65	6H-5, 5-10	45.85	46.00	2,990	13.2	1.19	8.91
5H-6, 5-10	40.65	47.85	9,376	35.9	3.46	27.62	6H-5, 30-35	46.10	46.25	3,293	10.6	0.79	8.16
5H-6, 80-85	41.40	48.87	6,804	30.4	3.21	28.37	6H-5, 80-85	46.60	46.75	5,240	18.9	1.96	17.50
5H-7, 5-10	42.15	49.85	6,633	27.1	2.65	21.30	6H-5, 105-110	46.85	47.00	4,223	18.8	1.61	14.85
6H-1, 5-10	42.65	50.45	6,346	30.3	2.90	23.47	6H-6, 5-10	47.35	47.50	7,851	36.0	3.70	24.72
6H-1, 81-86	43.41	51.21	5,496	24.2	2.15	18.34	6H-6, 30-35	47.60	47.75	8,116	35.8	3.28	26.90
6H-2, 5-10	44.15	52.08	15,270	44.6	3.89	31.83	6H-6, 80-85	48.10	48.25	7,864	32.5	3.31	29.07
6H-2, 80-85	44.90	52.92	12,540	41.9	4.42	38.32	6H-7, 5-10	48.85	49.00	6,362	32.0	3.11	27.55
6H-3, 5-10	45.65	53.59	15,550	48.4	4.54	42.79	7H-1, 5-10	49.35	50.51	5,745	26.2	2.58	21.12
6H-3, 80-85	46.40	54.27	14,170	53.9	4.46	42.18	7H-1, 80-85	50.10	51.54	10,640	44.8	3.40	25.46
6H-4, 5-10	47.15	54.94	10,440	53.2	4.79	46.60	7H-2, 5-10	50.85	52.56	14,430	40.6	4.49	31.96
6H-4, 80-85	47.90	55.46	4,203	84.8	4.57	36.35	7H-2, 80-85	51.60	53.35	12,340	42.2	4.50	40.64
6H-5, 5-10	48.65	56.25	1,319	168.2	6.09	36.84	7H-3, 5-10	52.35	54.10	12,090	52.2	4.01	37.27
6H-5, 30-35	48.90	59.04	695	114.8	5.56	30.78	7H-3, 80-85	53.10	54.85	8,963	49.7	4.82	46.29
6H-5, 81-86	49.41	59.55	723	233.9	7.71	41.82	7H-3, 105-110	53.35	55.10	9,473	52.1	4.16	42.14
6H-5, 105-110	49.65	62.40	***	260.3	8.43	42.12	7H-3, 130-135	53.60	55.35	5,372	64.0	4.11	34.99
6H-6, 5-10	50.15	62.90	941	320.6									

Table 3 (continued).

Core, section, interval (cm)	Depth (mbsf)	Depth (mcd)	Ba (ppm)	La (ppm)	Fe (%)	Sc (ppm)
7H-2, 5-10	55.85	54.20	15,560	54.6	4.33	39.54
7H-2, 80-85	56.60	54.59	9,501	50.0	4.61	45.00
7H-3, 5-10	57.35	55.00	11,240	49.2	4.64	42.03
7H-3, 80-85	58.10	55.50	4,282	87.3	4.62	36.85
7H-4, 5-10	58.85	56.25	979	101.5	4.71	29.89
7H-4, 80-85	59.60	57.00	873	82.1	4.57	36.82
7H-5, 5-10	60.35	57.75	823	78.6	4.65	33.40
7H-5, 80-85	61.10	58.50	408	85.2	4.87	33.57
7H-6, 5-10	61.85	59.25	505	89.8	5.52	30.36
7H-6, 30-35	62.10	59.50	569	137.2	5.38	34.17
7H-6, 80-85	62.60	60.00	***	130.7	6.40	37.38
7H-6, 105-110	62.85	60.25	***	158.1	5.96	36.78
7H-7, 5-10	63.35	60.75	934	112.9	4.92	29.14
7H-7, 30-35	63.60	61.00	***	117.7	5.12	32.40
8H-1, 5-10	63.85	62.00	467	248.3	8.98	40.26
8H-1, 30-35	64.10	62.25	***	283.7	11.48	43.23
8H-1, 80-85	64.60	62.75	718	212.4	11.56	38.82
8H-1, 105-110	64.85	63.00	553	234.2	12.49	38.14
8H-2, 5-10	65.35	63.50	730	193.0	13.86	32.02
8H-2, 30-35	65.60	63.75	734	199.9	14.44	31.15
8H-2, 80-85	66.10	64.25	656	197.1	16.50	31.11
8H-2, 105-110	66.35	64.50	1,277	225.9	18.46	31.64
8H-3, 5-10	66.85	65.00	1,103	251.8	20.13	30.11
8H-3, 30-35	67.10	65.25	***	276.8	21.78	30.77
8H-3, 80-85	67.60	65.75	1,455	272.9	28.39	28.59
8H-4, 5-10	68.35	66.50	1,126	584.8	29.42	31.79
8H-4, 80-85	69.10	67.25	1,923	497.3	27.24	24.23
8H-4, 105-110	69.35	67.50	1,819	482.4	27.70	24.44
8H-5, 5-10	69.85	68.00	1,964	358.8	27.45	20.56
8H-5, 30-35	70.10	68.25	1,941	341.0	27.48	19.36
8H-5, 80-85	70.60	68.75	1,887	360.4	25.76	20.98
8H-5, 105-110	70.85	69.00	1,677	363.8	25.98	21.30
8H-6, 5-10	71.35	69.50	4,051	184.6	32.25	9.49
8H-6, 30-35	71.60	69.75	2,630	173.8	30.33	11.56
8H-6, 80-85	72.10	70.25	2,611	293.4	23.75	18.32

Notes: Values have not been rounded to reflect significant digits. Triple asterisks (***) = below detection limit.

(between 62 and 69.5 mcd) is a relatively continuous sedimentary record, and that the lowermost hiatus at Hole 885A is not present at Hole 886C. Stepwise drops in the rate of hydrothermal accumulation (as at Hole 885A) would be expected if the record at Hole 886C contained a time interval(s) of significant nondeposition.

The composite depth scale also can be used to revise depths of lithologic boundaries at Sites 885/886. Sediment at these sites has been divided into three basic lithologic units (Rea, Basov, Janecek, Palmer-Julson, et al., 1993): Unit I is composed predominantly of clay, Unit II is composed primarily of diatom ooze, and Unit III consists of clay with variable amounts of Fe-Mn oxyhydroxides. On the basis of shipboard smear-slide analyses, the Unit I/II boundary was placed at approximately 14.1 mbsf at Hole 885A, 25.3 mbsf at Hole 886B, and 17.1 mbsf at Hole 886C, and the Unit II/III boundary was placed at approximately 45.8 mbsf at Hole 885A, 52.3 mbsf at Hole 886B, and 54.3 mbsf at Hole 886C. Although the latter boundary is stratigraphically equivalent (Table 1), the suggested Unit I/II boundary occurs at significantly different composite depths within each of Holes 885A, 886B, and 886C. This discrepancy likely reflects the low sampling resolution taken for smear-slide analyses at Sites 885/886 (1 to 3 samples per core), rather than differential sedimentation at the three holes. The Unit I/II boundary therefore has been realigned in Figure 5, such that it occurs at the same composite depth within holes at Sites 885/886. The depth of this boundary has been placed at approximately 23.8 mcd because this depth is where downcore variations in bulk chemistry (Table 3, Fig. 4) display the greatest change (it is assumed that variations in bulk Fe, La, and Sc within Units I and II primarily reflect changes in the proportion of clay to

biogenic silica). Finally, Unit III should be divided into Subunits IIIA and IIIB (Fig. 5) to stress that the lowermost sediment of this unit (>62 mcd) predominantly is composed of hydrothermally derived Fe-Mn oxyhydroxide precipitates (as evident in the downcore Fe profile, Fig. 4, and discussed in Dickens and Owen, this volume).

CONCLUSIONS

A composite sedimentary record for Sites 885 and 886 can be constructed from splices of Holes 885A, 886A, 886B, and 886C such that isochronous datums and changes in various physiochemical parameters at each hole occur at common depth horizons. This composite record (Fig. 6) implies recovery gaps ranging from 0.05 to 2.70 m, and coring overlaps ranging from 0.15 to 3.60 m. It suggests the existence of intervals that are significantly compressed and/or contain prominent hiatuses that occur in one hole but not in other holes. To avoid recovery gaps and/or certain hiatuses, we suggest that future sampling should be conducted according to Table 5.

ACKNOWLEDGMENTS

Shannon Miller and Ed Birdsall provided significant help with sample preparation for INAA analyses. We are very grateful to T.K. Hagelberg, N.G. Piasias, and T.C. Moore, Jr., for valuable comments based on an early version of this manuscript. Funding for G. Dickens was furnished by the U.S. Department of Energy under appointment to Graduate Fellowships for Global Change administered by Oak Ridge Institute for Science and Education (ORISE).

REFERENCES*

- Browne, E., and Firestone, R.B., 1986. *Table of Radioactive Isotopes*: New York (Wiley).
- Dickens, G.R., and Owen, R.M., 1993. Chinook Trough rifting and late Cretaceous hydrothermal deposition at ODP Site 886. *Eos*, 74:355. (Abstract)
- Hagelberg, T., Shackleton, N., Piasias, N., and Shipboard Scientific Party, 1992. Development of composite depth sections for Sites 844 through 854. In Mayer, L., Piasias, N., Janecek, T., et al., *Proc. ODP, Init. Repts.*, 138 (Pt. 1): College Station, TX (Ocean Drilling Program), 79-85.
- Hagelberg, T.K., Piasias, N.G., Shackleton, N.J., Mix, A.C., and Harris, S., 1995. Refinement of a high-resolution, continuous sedimentary section for studying equatorial Pacific Ocean paleoceanography, Leg 138. In Piasias, N.G., Mayer, L.A., Janecek, T.R., Palmer-Julson, A., and Van Andel, T.H. (Eds.), *Proc. ODP, Sci. Results*, 138: College Station, TX (Ocean Drilling Program), 31-46.
- Heath, G.R., Kovar, R.B., Lopez, C., and Campi, G.L., 1985. Elemental composition of Cenozoic pelagic clays from Deep Sea Drilling Project Sites 576 and 578, western North Pacific. In Heath, G.R., Burckle, L.H., et al., *Init. Repts. DSDP*, 86: Washington (U.S. Govt. Printing Office), 605-646.
- Murray, D.W., and Prell, W.L., 1991. Pliocene to Pleistocene variations in calcium carbonate, organic carbon, and opal on the Owen Ridge, northern Arabian Sea. In Prell, W.L., Niitsuma, N., et al., *Proc. ODP, Sci. Results*, 117: College Station, TX (Ocean Drilling Program), 343-363.
- Rea, D.K., Basov, I.A., Janecek, T.R., Palmer-Julson, A., et al., 1993. *Proc. ODP, Init. Repts.*, 145: College Station, TX (Ocean Drilling Program).

* Abbreviations for names of organizations and publications in ODP reference lists follow the style given in *Chemical Abstracts Service Source Index* (published by American Chemical Society).

Date of initial receipt: 4 April 1994
 Date of acceptance: 10 August 1994
 Ms 145SR-144

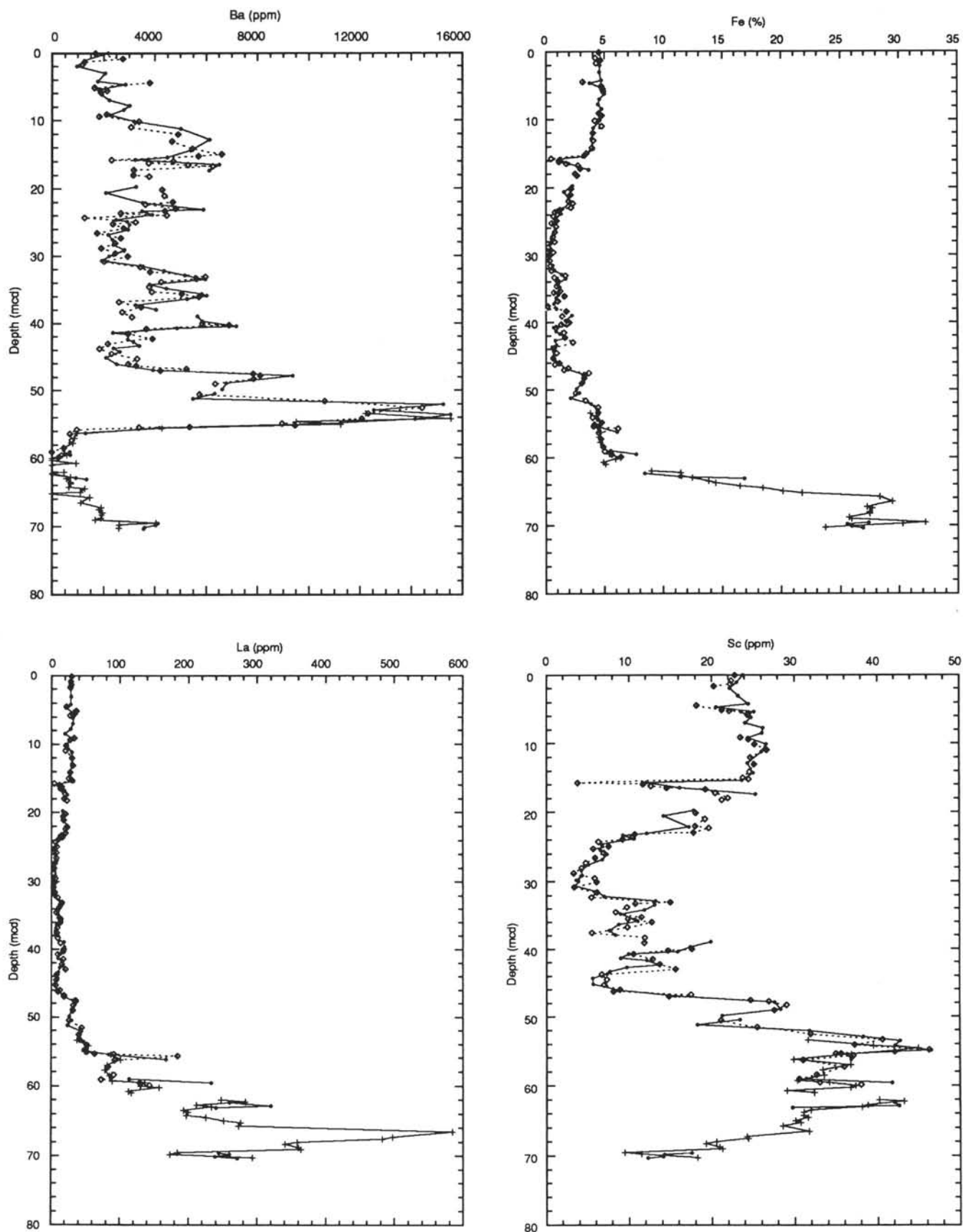


Figure 4. Downcore variations in bulk Ba, Fe, La, and Sc at Holes 885A (solid diamonds), 886B (open diamonds), and 886C (plus signs) plotted according to the composite depth scale (mcd). Breaks in records indicate coring gaps or hiatuses. Note depth offsets between 12 and 15 mcd, 20 and 22 mcd, and at approximately 30 mcd (discussed in text). Concentrations of Ba that are below the detection limit (between 59.08 and 65.25 mcd; see Table 2) are shown as zero.

Table 4. Stratigraphic implications of hole intercorrelation at Sites 885/886.

Hole 885A				Hole 886A			Hole 886B				Hole 886C			
Upper depth (mbsf)	Lower depth (mbsf)		Length (m)	Upper depth (mbsf)	Lower depth (mbsf)	Length (m)	Upper depth (mbsf)	Lower depth (mbsf)	Length (m)	Upper depth (mbsf)	Lower depth (mbsf)	Length (m)		
4.60	4.60	Overlap	-0.20	0.00	0.75	Core top ^a	1.80	1.80	Recovery gap	2.55	4.80	6.10	Hiatus	1.25
9.75	15.85	Compressed	3.75 ^b	9.70		End of hole	2.60	10.25	Unknown ^c	-7.50	6.80	6.80	Recovery gap	0.10
14.10	14.10	Recovery gap	1.85 ^b				11.30	11.30	Recovery gap	2.85	16.30	16.30	Overlap	-3.60
23.60	23.60	Overlap ^d	-1.15				20.80	20.80	Recovery gap	0.95	25.80	25.80	Overlap	-0.70
33.10	33.10	Recovery gap	0.55				28.80	30.30	Not recovered	(1.50)	35.30	35.30	Recovery gap	0.85
42.60	42.60	Overlap	-0.10				30.30	30.30	Overlap ^d	-0.75	39.80	44.80	Not recovered	(5.00)
48.65	48.70	Hiatus	1.90				39.80	39.80	Recovery gap	0.45	44.80	44.80	Recovery gap	0.20
49.41	49.55	Hiatus	2.60				49.30	49.30	Recovery gap	1.25	54.30	54.30	Overlap ^e	-0.50
50.40	50.65	Hiatus	5.95				58.80		End of hole ^f		63.80	63.80	Recovery gap	0.75 ^g
52.10		End of hole ^f									72.40		End of hole ^f	

Notes: "Length" column is the amount of sediment "missing" from (positive values) or "added" to (negative values) composite sedimentary record. Values in parentheses do not account for "missing" sediment.

^aAmount of sediment either not recovered (missing core top) and/or compressed relative to the composite depth scale.

^bCompressed interval and recovery gap together represent 5.60 m of depth offset (see text).

^cThe middle of Core 145-886B-2H contains approximately 7.50 m of sediment of unknown origin (see text).

^dCoring overlaps at approximately 30 mcd may alternatively reflect compression at Hole 886C (see text).

^eSediment in Section 145-886C-6H-1 is highly disturbed and may account for some of the coring overlap.

^fDepth of lowermost recovered sediment.

^gThe 0.75-m "gap" between Cores 145-886C-7H and -8H is an arbitrary value (see text).

Table 5. Suggested composite record for Sites 885/886.

Depth (mcd)	Splice	
	Hole, core	Interval (mbsf)
0.00-4.10	886C-1H	0.00-4.10
4.10-9.35	886A-1H	2.60-7.85
9.35-14.45	886C-2H	8.00-13.10
14.45-17.50	886B-3H	16.10-19.15
17.50-22.55	886C-3H	19.40-24.45
22.55-28.55	885A-3H	15.85-21.85
28.55-32.10	886C-4H ^a	30.15-33.70
32.10-39.40	886B-5H	32.40-39.70
39.40-40.55	885A-5H	33.60-34.75
40.55-47.65	886B-6H	40.40-47.50
47.65-52.70	886C-6H	49.05-54.10
52.70-55.35	886B-7H	50.95-53.60
55.35-basalt	886C-7H, -8H	57.95-72.40

^aBecause of intercorrelation problems across this interval, samples also might be taken from lowermost Core 145-885A-3H and uppermost Core 145-885A-4H.

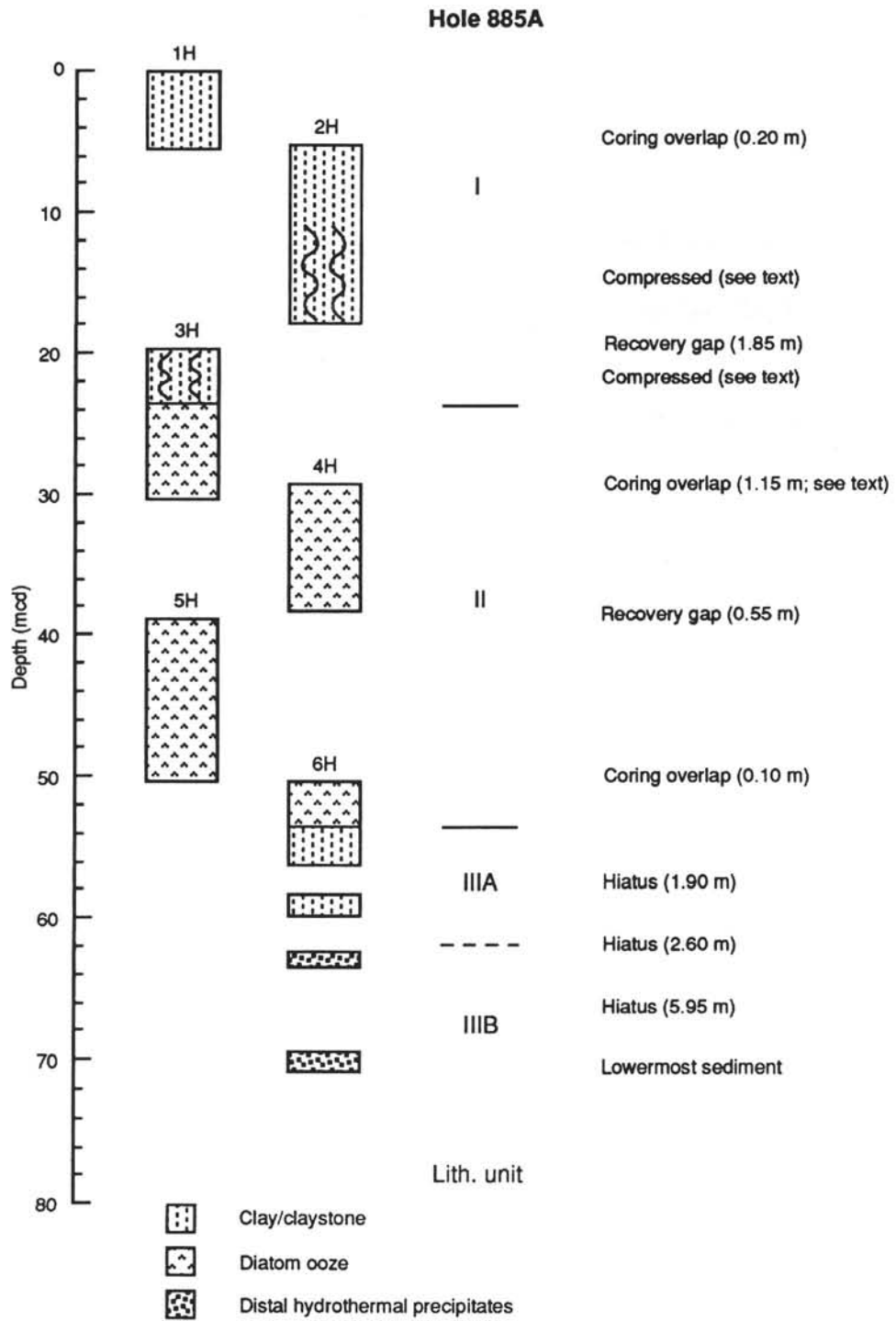


Figure 5. Core descriptions for Holes 885A, 886A, 886B, and 886C according to composite depth. The stratigraphic implications of the composite depth scale are listed to the right of each figure, and the revised lithologic description (see text) is displayed in the middle of each figure.

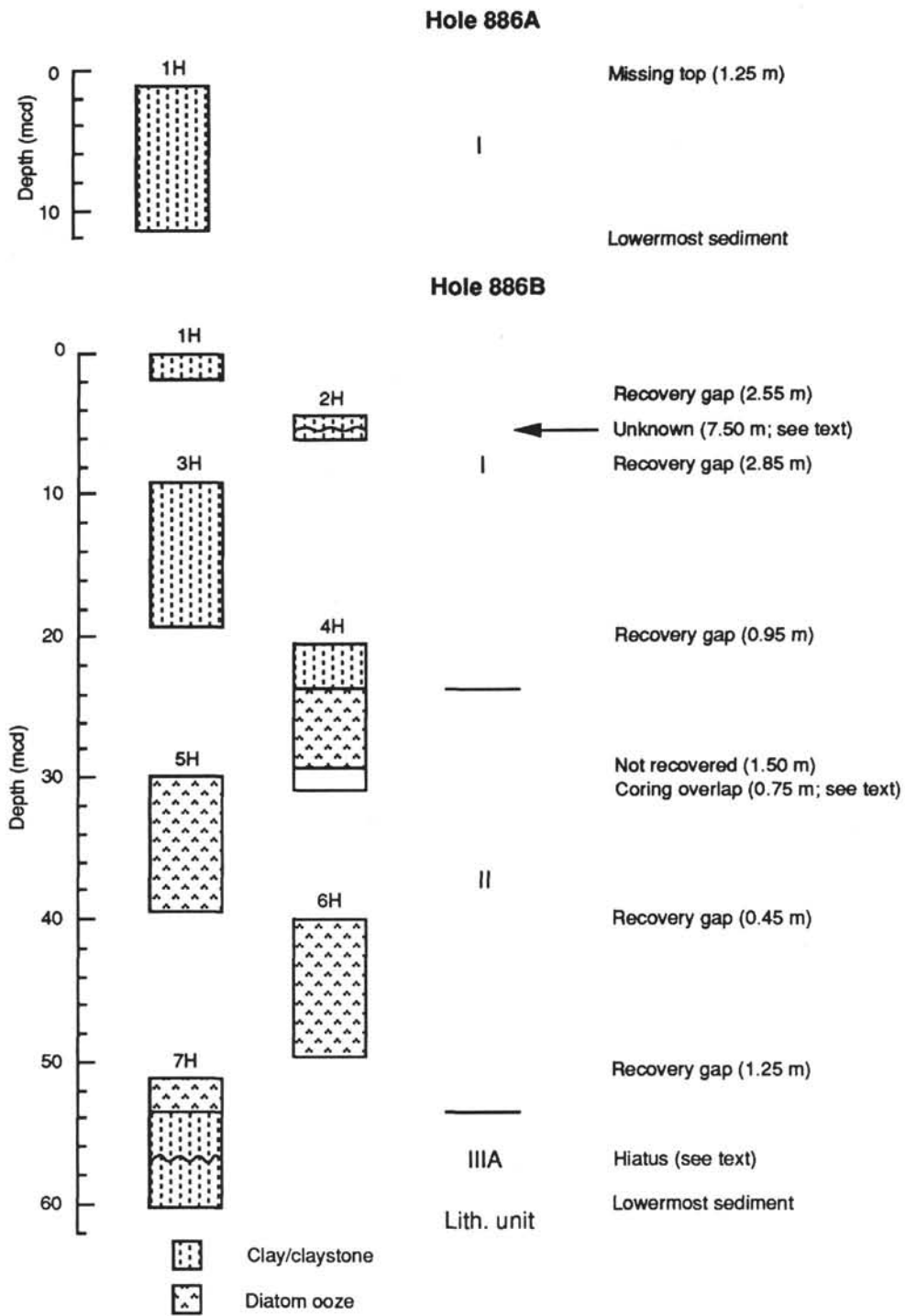


Figure 5 (continued).

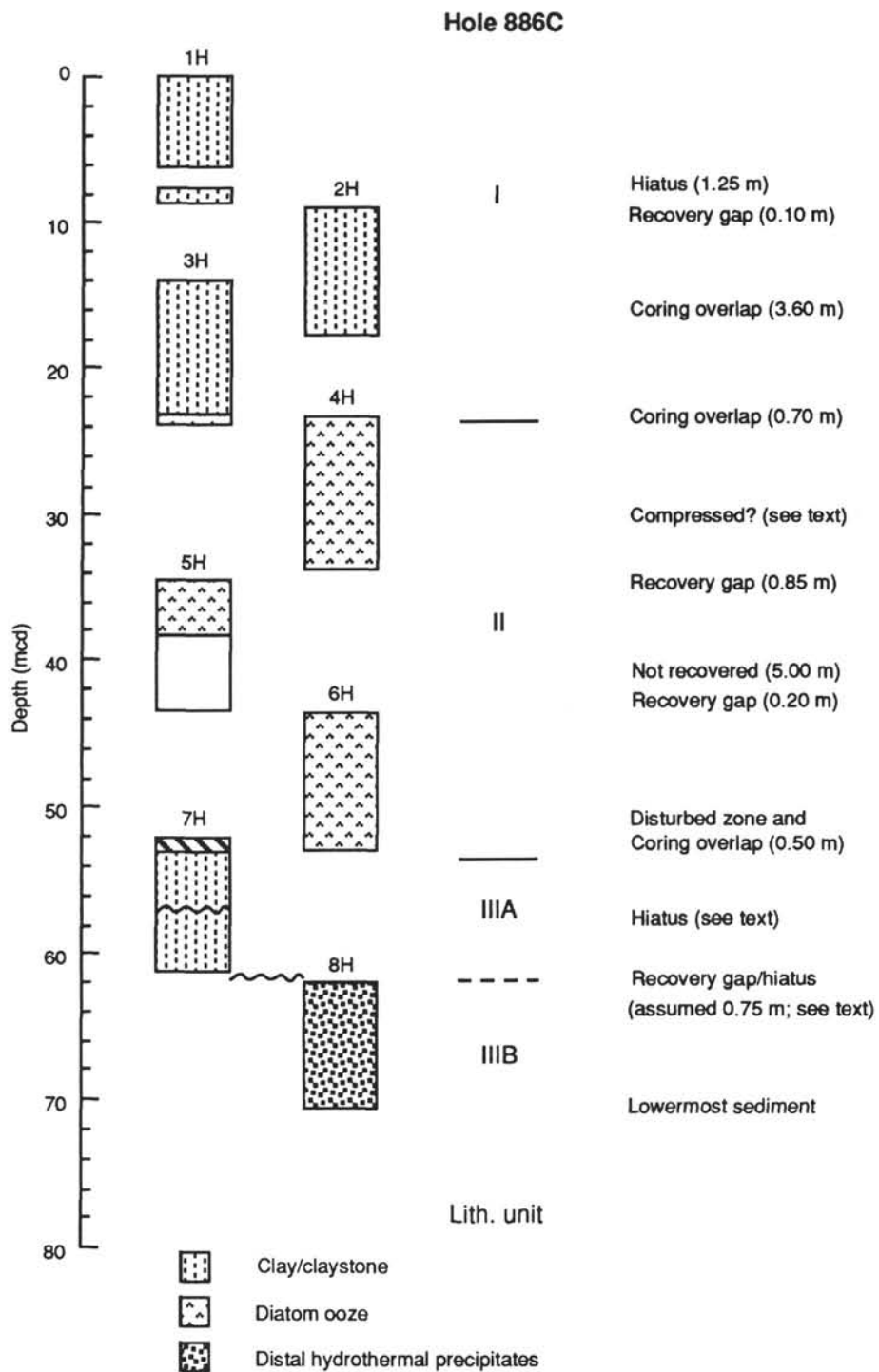


Figure 5 (continued).

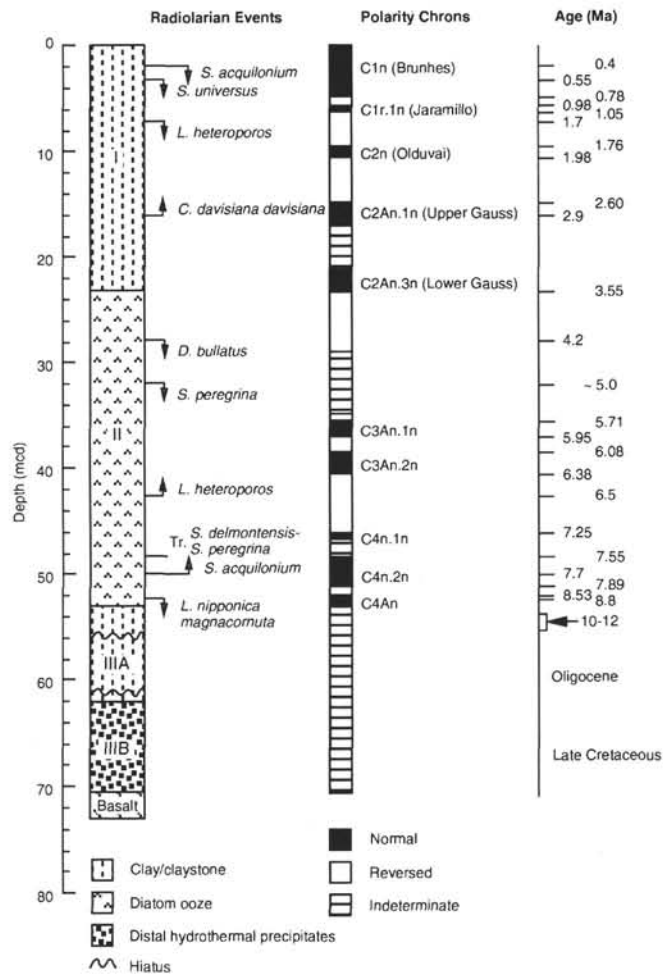


Figure 6. The composite stratigraphic record at Sites 885/886 with ages and approximate depth positions of isochronous radiolarian events and polarity chron boundaries (Table 2).